Biochem. J. (2013) **451**, 177–184 (Printed in Great Britain) doi:10.1042/BJ20121600

Subtype-selective regulation of IP_3 receptors by thimerosal via cysteine residues within the IP_3-binding core and suppressor domain

Samir A. KHAN*[1], Ana M. ROSSI*[1], Andrew M. RILEY†, Barry V. L. POTTER† and Colin W. TAYLOR*[2]

*Department of Pharmacology, Tennis Court Road, Cambridge CB2 1PD, U.K., and †Wolfson Laboratory of Medicinal Chemistry, Department of Pharmacy and Pharmacology, University of Bath, Claverton Down, Bath BA2 7AY, U.K.

IP_3R (IP_3 [inositol 1,4,5-trisphosphate] receptors) and ryanodine receptors are the most widely expressed intracellular Ca^{2+} channels and both are regulated by thiol reagents. In DT40 cells stably expressing single subtypes of mammalian IP_3R, low concentrations of thimerosal (also known as thiomersal), which oxidizes thiols to form a thiomercurylethyl complex, increased the sensitivity of IP_3-evoked Ca^{2+} release via IP_3R1 and IP_3R2, but inhibited IP_3R3. Activation of IP_3R is initiated by IP_3 binding to the IBC (IP_3-binding core; residues 224–604) and proceeds via re-arrangement of an interface between the IBC and SD (suppressor domain; residues 1–223). Thimerosal (100 μM) stimulated IP_3 binding to the isolated NT (N-terminal; residues 1–604) of IP_3R1 and IP_3R2, but not to that of IP_3R3. Binding of a competitive antagonist (heparin) or partial agonist (dimeric-IP_3) to NT1 was unaffected by thiomersal, suggesting that the effect of thimerosal is specifically related to IP_3R activation. IP_3 binding to NT1 in which all cysteine residues were replaced by alanine was insensitive to thimerosal, so too were NT1 in which cysteine residues were replaced in either the SD or IBC. This demonstrates that thimerosal interacts directly with cysteine in both the SD and IBC. Chimaeric proteins in which the SD of the IP_3R was replaced by the structurally related A domain of a ryanodine receptor were functional, but thimerosal inhibited both IP_3 binding to the chimaeric NT and IP_3-evoked Ca^{2+} release from the chimaeric IP_3R. This is the first systematic analysis of the effects of a thiol reagent on each IP_3R subtype. We conclude that thimerosal selectively sensitizes IP_3R1 and IP_3R2 to IP_3 by modifying cysteine residues within both the SD and IBC and thereby stabilizing an active conformation of the receptor.

Key words: Ca^{2+} channel, IP_3 receptor, IP_3-binding core, redox regulation, ryanodine receptor, suppressor domain, thimerosal (thiomersal), thiol.

INTRODUCTION

IP_3Rs [IP_3 (inositol 1,4,5-trisphosphate) receptors] and RyRs (ryanodine receptors) are related families of intracellular Ca^{2+} channels (see Supplementary Figure S1 at http://www.biochemj.org/bj/451/bj4510177add.htm). IP_3Rs are expressed in most animal cells [1] and RyRs are expressed in many cells, but most abundantly in excitable tissues [2]. Most IP_3Rs and RyRs are expressed within the membranes of the endoplasmic or sarcoplasmic reticulum, where they mediate the release of Ca^{2+} stored within them. Vertebrate genomes have three genes for IP_3R subunits and most have three genes for RyR. Functional intracellular Ca^{2+} channels are tetrameric assemblies of these very large subunits, probably only homotetramers for RyR [2] (but see [3]), whereas IP_3R form both homo- and hetero-tetrameric channels [1]. Activation of IP_3R is initiated by binding of IP_3 to the IBC (IP_3-binding core; residues 224–604) of each IP_3R subunit [4] and then proceeds via re-arrangement of an interface between the IBC and SD (suppressor domain; residues 1–223) [5,6] (see Supplementary Figure S1). The links between these conformational changes within the NT (N-terminal residues 1–604) domains of the IP_3R and gating of the channel formed by transmembrane helices close to the C-terminal are poorly understood, but they are known to require the SD [7].

The two families of intracellular Ca^{2+} channels, IP_3Rs and RyRs, share many characteristics including related structures [6], similar pores [8] and many aspects of their regulation. The latter includes regulation by cytosolic Ca^{2+} [9,10] and modulation by thiol-reactive reagents [11,12]. Indeed, modification of cysteinyl residues within ion channels is widespread [13–17], and contributes both to pathological responses to oxidative stress [18] and to physiological signals, including nitric oxide [19], hydrogen peroxide [20] and oxygen [21], which generate reactive oxygen or nitrogen species (see references in [22]).

Thimerosal (also known as thiomersal) was once widely used as an antiseptic and as a preservative, particularly in childhood vaccines, but after considerable controversy it is now rarely used [23]. However, as a membrane-permeable thiol-oxidizing agent, thimerosal remains a useful experimental tool that interacts with free thiol groups to form a thiomercuryethyl complex. Many studies have reported thimerosal-evoked increases in cytosolic Ca^{2+} concentration and suggested that they, at least partly, result from its effects, whether direct or via oxidation of GSH, on IP_3Rs or RyRs (reviewed in [24]).

Many thiol reagents, including thimerosal [25], biphasically regulate RyR activity: low concentrations stimulate activity, whereas higher concentrations are inhibitory [12,22]. This pattern is reminiscent of the biphasic regulation of RyR by cytosolic Ca^{2+} [10], and consistent with evidence that oxidation of critical cysteine residues increases the sensitivity of RyRs to endogenous regulators [26] (reviewed in [12]). There are approximately 100 cysteine residues in each RyR subunit and within the reducing

Abbreviations used: CLM, cytosol-like medium; GST, glutathione transferase; IBC, inositol 1,4,5-trisphosphate-binding core; IP_3, inositol 1,4,5-trisphosphate; IP_3R, inositol 1,4,5-trisphosphate receptor; K_d, equilibrium dissociation constant; KO, knockout; NT, N-terminal; $NT1^{CL}$, cysteine-less NT1; $NT1^{CL-IBC}$, NT1 where cysteine residues within the IBC were replaced by alanine; $NT1^{CL-SD}$, NT1 where cysteine residues within the SD were replaced by alanine; RyR, ryanodine receptor; RyR1A, A domain of the type 1 RyR; RyR2A, A domain of the type 2 RyR; SD, suppressor domain.

[1] These authors contributed equally to this work.

[2] To whom correspondence should be addressed (email cwt1000@cam.ac.uk).

environment of the cytosol approximately half of these are in the reduced state [22]. A few of these residues are particularly susceptible to oxidation, and their susceptibility depends on whether the RyR is open or closed. But there is not yet any clearly defined relationship between oxidation of specific cysteine residues and channel activity (reviewed in [12]).

An abundant amount of evidence demonstrates that IP_3R activity is also modulated by thiol-oxidizing agents [27] (reviewed in [11]). In many cells, for example, the effects of thimerosal on IP_3-evoked Ca^{2+} release are rather similar to its biphasic effects on RyRs: potentiation of responses at low concentrations and inhibition of Ca^{2+} release at higher concentrations of thimerosal [11]. Although the responses to thimerosal in intact cells are undoubtedly made more complicated by its effects on additional Ca^{2+}-handing proteins and perturbation of GSH/GSSG [28], there are clearly direct biphasic effects on IP_3R behaviour [29] (see references in [11]). There are 60 cysteine residues in each IP_3R1 subunit and most are likely to be in the reduced form in their native setting [11]. None of the 12 cysteine residues within the S1 splice variant of the IP_3R1 NT are required for effective gating of IP_3Rs by IP_3 [6], but two conserved cysteine residues within the C-terminal tail (Cys^{2610} and Cys^{2613}) are essential [7], and three reduced cysteine residues within the third luminal loop of IP_3R1 (Cys^{2496}, Cys^{2504} and Cys^{2527}) are essential for its redox-sensitive interaction with a luminal thioredoxin-related protein, ERp44 [30]. The mechanisms whereby thimerosal or other thiol reagents modulate IP_3R behaviour have not been resolved, but they are relevant to understanding redox regulation of IP_3Rs under physiological and pathological conditions, and to defining further the mechanisms of IP_3R activation. The mechanism by which thimerosal regulates the three subtypes of IP_3Rs is addressed in the present study.

MATERIALS AND METHODS

Materials

Thimerosal and heparin (sodium salt from bovine intestinal mucosa) were from Sigma–Aldrich. IP_3 was from Enzo Life Sciences (Exeter). [^{3}H]IP_3 (18 Ci/mmol) was from PerkinElmer Life and Analytical Sciences. Dimeric IP_3 (structure shown in Figure 3A) was synthesized and characterized as reported previously [5]. Sources of other materials are specified in previous publications [31,32] or within the relevant methods sections.

Expression of NT fragments of IP_3 receptors

NT fragments of rat IP_3R1 (NT1 and IBC) (Supplementary Table S1 at http://www.biochemj.org/bj/451/bj4510177add.htm) were amplified by PCR from the full-length coding sequence of IP_3R1 lacking the S1 splice site (GenBank accession number: GQ233032.1) and ligated into pGEX-6P-2 vectors (GE Healthcare). The open reading frame encoding NT2 (residues 1–604 from mouse IP_3R2) (GenBank: GU980658.1) and NT3 (residues 1–604 from rat IP_3R3) (GenBank: GQ233031.1) were amplified by PCR using the primers listed in Supplementary Table S2 (at http://www.biochemj.org/bj/451/bj4510177add.htm). PCR products were digested with SmaI and XhoI and ligated into pGEX-6P-2 vectors for expression in *Escherichia coli*. The methods used to express an $NT1^{CL}$ (cysteine-less NT1) in which all endogenous cysteine residues of the NT of IP_3R1 were replaced by alanine, and a chimaeric NT (RyR2A-IBC) in which the A domain of the type 2 RyR (RyR2; residues 1–210) (GenBank: GI164831) [33] was fused to the IBC of rat IP_3R1 were described recently [6]. The plasmid encoding $NT1^{CL-IBC}$ (NT1 where cysteine residues within the IBC were replaced by alanine) (Supplementary Table S1) was generated from the NT1 construct using QuikChange multi-site-directed mutagenesis (Agilent). The $NT1^{CL}$ construct was used as the template to prepare a plasmid encoding $NT1^{CL-SD}$ (NT1 where all endogenous cysteine residues within the SD were replaced by alanine) (Supplementary Table S1). The sequence encoding the cysteine-less SD was PCR-amplified from the $NT1^{CL}$ template using the primers listed in Supplementary Table S2. PCR products were then ligated into the pET41a(+) vector containing the open reading frame of the IBC of IP_3R1 as SpeI/EcoRV fragments for expression in *E. coli*. The coding sequences of all expression constructs were confirmed. Supplementary Table S1 lists the proteins used and their abbreviations.

All N-terminal fragments of IP_3R were expressed as fusion proteins linked to N-terminal GST (glutathione transferase) via a PreScission cleavage site in *E. coli* BL21 (DE3) exactly as described previously [32]. Bacteria were harvested (6000 ***g*** for 15 min at 4 °C), washed twice with phosphate-buffered saline and stored at −80 °C before purification of the fragments. Bacterial pellets were suspended (1 g/10 ml) in Tris-buffered medium [50 mM Tris and 1 mM EDTA (pH 8.3)] and lysed by incubation with 100 μg/ml lysozyme (Sigma–Aldrich), 5 units/ml DNase (Sigma–Aldrich) and 10 μg/ml RNase (Sigma–Aldrich) for 1 h on ice, followed by sonication (30 s). After centrifugation (30000 ***g*** for 60 min at 4 °C), the supernatant was mixed with glutathione–Sepharose 4B beads [GE Healthcare; lysate/beads (v/v) 50:1) and incubated with gentle rotation for 1 h at 20 °C. The beads were then washed with Tris-buffered medium supplemented with 1 mM dithiothreitol, centrifuged (500 ***g*** for 5 min at 4 °C) and incubated in the same medium (1 ml) supplemented with 160 units/ml GST-tagged PreScission protease (GE Healthcare) for 16 h at 4 °C with gentle rotation. After centrifugation (500 ***g*** for 5 min at 4 °C), the NT fragments, cleaved from their GST tags, were recovered in the supernatant and rapidly frozen in liquid nitrogen before storage at −80 °C. Immunoblots of the proteins used are shown in Supplementary Figure S3 (at http://www.biochemj.org/bj/451/bj4510177add.htm).

[^{3}H]IP_3 binding

Equilibrium competition binding assays were performed in Tris-buffered medium (500 μl) containing purified protein (1–5 μg), [^{3}H]IP_3 (0.25–0.75 nM) and appropriate concentrations of competing ligand. Where indicated, thimerosal was added 10 min before the addition of [^{3}H]IP_3. Reactions were terminated after 5 min by addition of poly(ethylene glycol)-8000 [Sigma–Aldrich; 30 % (w/v) 500 μl] and γ-globulin (Sigma–Aldrich; 750 μg in 30 μl of Tris-buffered medium). Bound and free [^{3}H]IP_3 were then separated by centrifugation (20000 ***g*** for 5 min). Results were fitted to Hill equations using GraphPad Prism (version 5.0, GraphPad) from which IC_{50}, and thereby K_d (equilibrium dissociation constant) and pK_d, values were calculated.

Ca^{2+} release from the intracellular stores of DT40 cells expressing IP_3R subtypes

DT40 cells, in which the genes for all three endogenous IP_3R subtypes had been disrupted [DT40-KO (knockout) cells], were used to generate stable cell lines expressing rat IP_3R1, mouse IP_3R2 or rat IP_3R3 (DT40-IP_3R1–3 cells) or a chimaeric IP_3R (RyR1A-IP_3R1) in which the SD of IP_3R1 was replaced by the equivalent A domain of rabbit type 1 RyR (RyR1; residues

1–210; GenBank accession number: X15209) (DT40-RyR1A-IP_3R1 cells) (Supplementary Table S1). The methods used to establish these stable cell lines have been described previously [6,34]. All DT40 cells were grown in suspension at 37 °C in an atmosphere of 95 % air and 5 % CO_2 in RPMI 1640 medium supplemented with 2 mM L-glutamine, 10 % fetal bovine serum, 1 % heat-inactivated chicken serum and 50 μM 2-mercaptoethanol. Cells were used or passaged when they reached a density of $\sim 2\times10^6$ cells/ml. Expression levels of IP_3Rs in the cell lines were compared by immunoblotting using antisera selective for each IP_3R subtype or an anti-peptide serum (AbC) that interacts equally with all three IP_3R subtypes. The immunoblotting methods were reported previously [34].

A low-affinity Ca^{2+} indicator, Mag-fluo-4, trapped within the endoplasmic reticulum, was used to measure luminal free Ca^{2+} concentration [31]. The endoplasmic reticulum of DT40 cells ($\sim 4\times10^6$ cells/ml) was loaded with indicator by incubating cells in the dark (for 1 h at 20 °C) with 20 μM Mag-fluo-4/AM (acetoxymethyl ester) in Hepes-buffered saline [135 mM NaCl, 5.9 mM KCl, 11.6 mM Hepes, 1.5 mM $CaCl_2$, 11.5 mM glucose and 1.2 mM $MgCl_2$ (pH 7.3)], supplemented with Pluronic F127 (1 mg/ml) and BSA (0.4 mg/ml). After centrifugation (650 ***g*** for 2 min), cells ($\sim 4\times10^6$ cells/ml) were suspended in Ca^{2+}-free CLM [cytosol-like medium; 140 mM KCl, 20 mM NaCl, 2 mM $MgCl_2$, 1 mM EGTA and 20 mM Pipes (pH 7.0)], supplemented with saponin (final concentration 20 μg/ml) to allow for selective permeabilization of the plasma membrane. After $\sim$4 min at 37 °C, when all cells had become permeable to 0.1 % Trypan Blue, the cells (5×10^5 cells/ml) were recovered (650 ***g*** for 2 min) and suspended at 20 °C in Mg^{2+}-free CLM, supplemented with $CaCl_2$ (375 μM, to provide a final free Ca^{2+} concentration of 220 nM after addition of 1.5 mM MgATP) and 10 μM FCCP (carbonyl cyanide *p*-trifluoromethoxyphenylhydrazone). The cells were then distributed into poly-L-lysine-coated 96-well plates (50 μl/well), centrifuged (300 ***g*** for 2 min) and used for fluorescence measurements. Fluorescence (excitation 485 nm, emission 520 nm, measured at 1.5 s intervals) was recorded at 20 °C using a FlexStation III plate-reader (Molecular Devices) [31]. MgATP (1.5 mM) was added to allow intracellular stores to sequester Ca^{2+}. After the stores had loaded to steady state ($\sim$150 s), IP_3 was added with thapsigargin (1 μM to inhibit Ca^{2+} re-uptake). Ca^{2+} release was measured after a further 60 s. The Ca^{2+} release evoked by IP_3 is expressed as a fraction of the ATP-dependent Ca^{2+} uptake [31]. Concentration–effect relationships were fitted to Hill equations using non-linear curve fitting (version 5.0, GraphPad Prism).

Statistical analyses of IP_3R sensitivity to IP_3 used pEC_{50} and pK_d values (negative logarithm of the EC_{50} and K_d respectively). Results are presented as means $\pm$ S.E.M. For clarity, mean EC_{50} and K_d values (derived from pEC_{50} or pK_d) are shown alongside. In paired comparisons of the effects of thimerosal, ΔpEC_{50} (or ΔpK_d) values are shown, where $\Delta pEC_{50} = EC_{50}{}^{\text{thimerosal}} - pEC_{50}{}^{\text{control}}$. Statistical analyses used ANOVA followed by paired Student's *t* test. $P < 0.05$ was considered significant.

RESULTS AND DISCUSSION

Thimerosal potentiates IP_3-evoked Ca^{2+} release via IP_3R1 and IP_3R2

In DT40 cells stably expressing only IP_3R1 (DT40-IP_3R1 cells) (Figure 1A), IP_3 caused a concentration-dependent release of Ca^{2+} from intracellular stores ($pEC_{50} = 7.95 \pm 0.04$) (Figure 1B). Pre-incubation with thimerosal (10 μM for 120 s) increased the sensitivity to IP_3 ($pEC_{50} = 8.95 \pm 0.31$, $\Delta pEC_{50} = 1.00 \pm 0.32$)

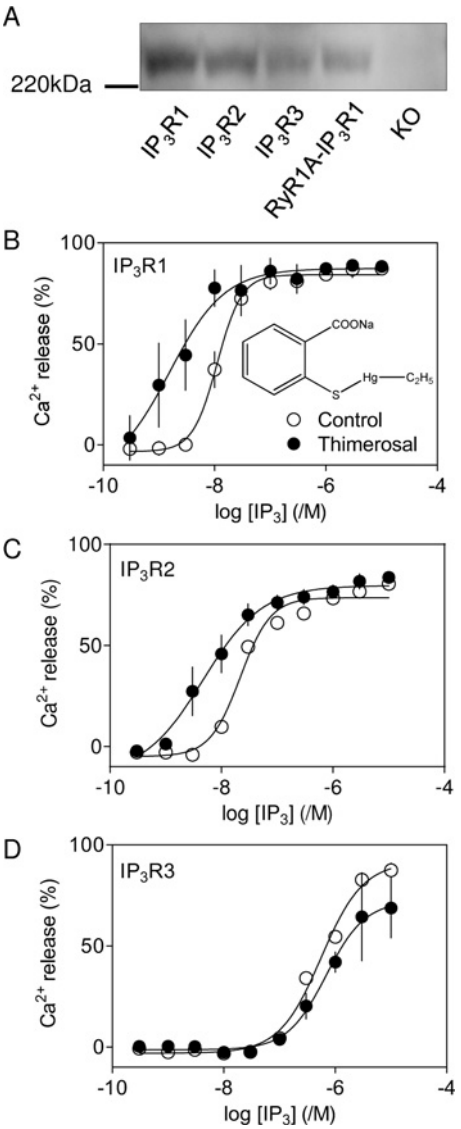

Figure 1 IP_3-evoked Ca^{2+} release via IP_3R1 and IP_3R2 is sensitized by thimerosal

(**A**) Immunoblot (4×10^4 cells/lane) using an antiserum (AbC) that recognizes a conserved NT sequence in all IP_3R subtypes demonstrates that expression levels of the three IP_3R subtypes and chimaeric IP_3R are broadly similar in each of the four cell lines. There are no detectable IP_3Rs in the DT40-KO cells. (**B**–**D**) Concentration-dependent effects of IP_3 on Ca^{2+} release are shown for control cells and after treatment with thimerosal (10 μM, 2 min) for DT40 cells expressing each of the three IP_3R subtypes. Results are means $\pm$ S.E.M. for at least three independent experiments. The structure of thimerosal is shown within (**B**). ○, control; ●, thimerosal.

without affecting loading of the Ca^{2+} stores or the maximal response to IP_3 (Table 1 and Figure 1B). Similar results were obtained with DT40 cells expressing only IP_3R2 (DT40-IP_3R2 cells) (Figure 1A), where 10 μM thimerosal also increased the sensitivity to IP_3 ($\Delta pEC_{50} = 0.60 \pm 0.20$) (Figure 1C). For both IP_3R1 and IP_3R2, higher concentrations of thimerosal inhibited responses to IP_3 (Table 1). However, in DT40 cells expressing IP_3R3 (DT40-IP_3R3 cells) (Figure 1A), 10 μM thimerosal inhibited IP_3-evoked Ca^{2+} release ($\Delta pEC_{50} = -0.17 \pm 0.01$) (Figure 1D), without significantly affecting loading of the intracellular Ca^{2+} stores (Table 1). The latter demonstrates that the diminished responses to IP_3 were not due to thimerosal activating IP_3R3 and thereby draining the Ca^{2+} stores before

Table 1 Effects of thimerosal on IP_3-evoked Ca^{2+} release by different IP_3Rs

DT40 cells expressing each of the IP_3R subtypes were incubated with the indicated concentrations of thimerosal during loading of the intracellular stores with Ca^{2+} (2 min) before addition of IP_3. Results show Ca^{2+} uptake (as a percentage of its value in the absence of thimerosal), maximal IP_3-evoked Ca^{2+} release (as a percentage of the Ca^{2+} content of the stores before addition of IP_3) and the Hill coefficient (h), pEC_{50} and EC_{50} values for the IP_3-evoked Ca^{2+} release. All results (except EC_{50}, which shows only the mean, see the Materials and methods section) are shown as means ± S.E.M. for three to four independent experiments. ND, not determined.

IP_3R subtypes	Thimerosal (μM)	Ca^{2+} uptake (%)	EC_{50} (nM)	pEC_{50}	h	Maximal Ca^{2+} release (%)
IP_3R1	0	100	11	7.95 ± 0.04	2.0 ± 0.1	84 ± 2
	1	98 ± 5	7	8.16 ± 0.13	1.2 ± 0.2	89 ± 1*
	10	97 ± 7	1	8.95 ± 0.31*	2.7 ± 0.8	85 ± 2
	100	93 ± 6	77	7.11 ± 0.18*	1.0 ± 0.4	42 ± 11*
IP_3R2	0	100	23	7.64 ± 0.01	1.6 ± 0.1	74 ± 2
	1	99 ± 2	14	7.87 ± 0.22	1.3 ± 0.2	78 ± 3
	10	96 ± 7	6	8.24 ± 0.26*	2.2 ± 0.3	77 ± 4
	100	93 ± 3	35	7.46 ± 0.28	0.9 ± 0.2	67 ± 2*
IP_3R3	0	100	576	6.24 ± 0.04	1.2 ± 0.1	88 ± 2
	1	99 ± 3	687	6.16 ± 0.08	1.0 ± 0.1	90 ± 5
	10	97 ± 8	860	6.07 ± 0.06*	1.3 ± 0.1	78 ± 8
	100	86 ± 6	2185	5.66 ± 0.02*	3.0 ± 0.5	54 ± 2*
RyR1A-IP_3R1	0	100	65	7.19 ± 0.01	2.4 ± 0.1	81 ± 4
	1	97 ± 4	78	7.11 ± 0.04	2.0 ± 0.2	76 ± 3
	10	89 ± 4	238	6.62 ± 0.18*	1.6 ± 0.2	80 ± 6
	100	66 ± 8*	ND	ND	ND	12 ± 1≠

*$P < 0.05$ relative to its control. ≠Response to 1 μM IP_3.

addition of IP_3. Functional effects of thimerosal were reported previously for DT40 cells expressing IP_3R1 or IP_3R3 [29], but use of the same single sub-threshold concentration of IP_3 for both IP_3R subtypes when IP_3R3 is much less sensitive to IP_3 (Figure 1 and Table 1) [35] compromised the conclusion that thimerosal sensitizes only IP_3R1. Our results, demonstrating that low concentrations of thimerosal sensitize IP_3R1 and IP_3R2 to IP_3 while inhibiting IP_3R3, are consistent with previous studies in which thimerosal [29,36–42] or other thiol reagents [40,43,44] potentiated IP_3-evoked Ca^{2+} signals in cells expressing predominantly IP_3R1 [29,37,42] or IP_3R2 [38,40,43,44], but not in cells where IP_3R3 predominates [29,39,41]. We conclude that within homotetrameric populations of IP_3R, thimerosal potentiates responses from IP_3R1 and IP_3R2, but inhibits IP_3R3.

Thimerosal stimulates IP_3 binding to the NTs of IP_3R1 and IP_3R2

Thimerosal stimulates IP_3-evoked Ca^{2+} release via purified IP_3R1 [37] and it stimulates [^{3}H]IP_3 binding to purified IP_3R1 [37] and its isolated NT [29]. This confirms that thimerosal directly affects IP_3R1. Activation of IP_3R is initiated by IP_3 binding to the IBC and proceeds via re-arrangement of interactions between the IBC and SD [6]. We therefore examined [^{3}H]IP_3 binding to the NTs of IP_3R1–IP_3R3, a region that comprises the critical SD and IBC (Supplementary Figure S1A).

Incubation (10 min) of purified NT from IP_3R1 (NT1) with thimerosal caused a concentration-dependent stimulation of [^{3}H]IP_3 binding that was maximal with 100 μM thimerosal and then reversed at higher concentrations (Figure 2A). A biphasic effect of thimerosal on [^{3}H]IP_3 binding to full-length IP_3R1 [45] and an NT region of IP_3R1 (residues 1–581) was reported previously [46]. The maximally effective concentration of thimerosal (100 μM) caused a 12-fold increase in the affinity of NT1 for IP_3 ($\Delta pK_d = 1.07 \pm 0.28$) (Figure 2B and Table 2). The effect of maximally effective concentrations of thimerosal (10–100 μM) on the sensitivities of functional responses of IP_3R1 to IP_3 ($\Delta pEC_{50} = 1.00 \pm 0.32$) and IP_3 binding to NT1 ($\Delta pK_d = 1.07 \pm 0.28$) are similar: both are increased ~10-fold. The results were similar with IP_3R2: 100 μM thimerosal caused a ~10-fold increase in the affinity of NT2 for IP_3 ($\Delta pK_d = 1.05 \pm 0.19$) (Figure 2C and Table 2). There was no significant effect of thimerosal on IP_3 binding to the NT of IP_3R3 (Figure 2D and Table 2).

Previous work suggested that thimerosal stimulates [^{3}H]IP_3 binding to full-length IP_3R1, but not to IP_3R3, whereas it stimulated binding to the NT region (residues 1–581) of IP_3R1 and IP_3R3, but not to that of IP_3R2 [29,46]. The previous conclusions are neither internally consistent nor consistent with our observations using NT1–NT3 (residues 1–604) (Figure 2). The residues missing in the shorter NT fragments are reasonably conserved between IP_3R subtypes and they lack cysteine residues (Supplementary Figure S1B). However, from the high-resolution structure of the IBC [4], an NT region truncated at residue 581 is likely to disrupt an α-helix (α9 in [4]), the NT of which forms essential interactions with IP_3. Furthermore, the published affinities for IP_3 of these shorter fragments from IP_3R1 and IP_3R3 are indistinguishable, which is inconsistent with evidence that in both NT and full-length proteins, IP_3R3 has lower affinity than IP_3R1 [35] (Table 2). It seems likely that the shorter fragments used in the previous studies [29,46] may not retain the native structure of the IBC.

Our results with [^{3}H]IP_3 binding to the NT from all three IP_3R subtypes (Figure 2), evidence from [^{3}H]IP_3 binding to full-length IP_3R1 and IP_3R3 expressed in Sf9 insect cells [29], our functional analyses of DT40 cells expressing homogenous populations of IP_3R subtypes (Figure 1) and substantial evidence from native cells expressing different IP_3R subtypes (discussed above) are consistent with the conclusion that low concentrations of thimerosal stimulate IP_3 binding and IP_3-evoked Ca^{2+} release via IP_3R1 and IP_3R2, but not via IP_3R3. These observations support the hypothesis that cysteine residues within the NT of IP_3R1 and IP_3R2 mediate the sensitizing effects of thimerosal on

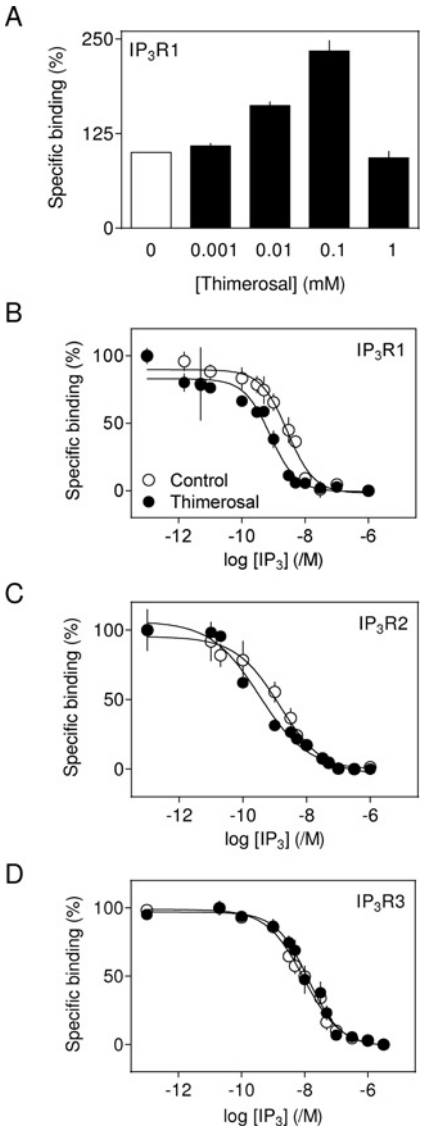

Figure 2 Thimerosal stimulates [^{3}H]IP_3 binding to the NT of IP_3R1 and IP_3R2

(**A**) Specific binding of [^{3}H]IP_3 (0.5 nM) to the NT of IP_3R1 is shown after pre-incubation (10 min) with the indicated concentrations of thimerosal. Results are shown as the percentage of specific [^{3}H]IP_3 binding measured in the absence of thimerosal. (**B**–**D**) Concentration-dependent effects of IP_3 on specific [^{3}H]IP_3 binding (0.5 nM) to the NT from each of the three IP_3R subtypes alone or after incubation with thimerosal (100 μM, 10 min). (**A**–**D**) Results are means $\pm$ S.E.M. for four independent experiments. ○, control; ●, thimerosal.

IP_3-evoked Ca^{2+} release. Subsequent experiments address this hypothesis.

Thimerosal stimulates agonist, but not antagonist, binding to the NT of IP_3R1

Heparin is a competitive antagonist of IP_3R [47], and dimeric IP_3 (see Figure 3A for structure) is a high-affinity partial agonist: the IP_3 dimer binds to the IP_3R, but causes lesser activation than IP_3 such that the channel opens less frequently [5]. Both heparin and IP_3 dimer completely displaced specifically bound [^{3}H]IP_3 from NT1, but thimerosal (100 μM, 10 min) affected the affinity of neither: ΔpK_d was 0.11 ± 0.09 and -0.06 ± 0.19 for heparin and IP_3 dimer respectively (Figure 3 and Table 3). These

Table 2 Effects of thimerosal on [^{3}H]IP_3 binding to the NT of each IP_3R subtype

Equilibrium-competition binding experiments using [^{3}H]IP_3 (0.5 nM) and NT1–NT3 show the effects of thimerosal (100 μM, 10 min) on the K_d (mean), pK_d (mean $\pm$ S.E.M.) and Hill coefficient (h, mean $\pm$ S.E.M.) for IP_3. $\Delta pK_d = pK_d^{thimerosal} - pK_d^{control}$. Results are from at least four independent experiments.

	pK_d (K_d; nM) h		
NT subtype	Control	Thimerosal	ΔpK_d
NT1	8.62 ± 0.10	9.69 ± 0.26*	1.07 ± 0.28
	(2.39)	(0.20)	
	1.2 ± 0.2	1.2 ± 0.3	
NT2	9.12 ± 0.07	10.17 ± 0.15*	1.05 ± 0.19
	(0.76)	(0.07)	
	0.6 ± 0.04	0.6 ± 0.02	
NT3	8.06 ± 0.06	7.91 ± 0.17	0.15 ± 0.22
	(8.72)	(12.4)	
	0.7 ± 0.06	1.0 ± 0.05	

*$P < 0.05$ relative to its control.

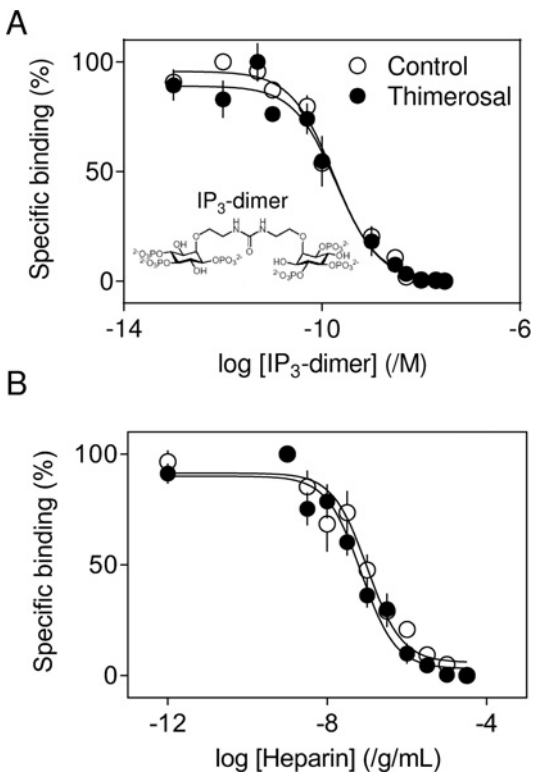

Figure 3 Thimerosal does not affect binding of an antagonist or partial agonist

(**A** and **B**) Concentration-dependent effects of the IP_3 dimer (**A**) or heparin (**B**) on specific [^{3}H]IP_3 binding (0.25 nM) to the NT from IP_3R1 alone or after incubation with thimerosal (100 μM, 10 min). Results are means $\pm$ S.E.M. for four independent experiments. The structure of the IP_3 dimer is shown within (**A**). ○, control; ●, thimerosal.

results are important because they demonstrate that thimerosal selectively affects the binding of ligands that activate IP_3R. It is, however, noteworthy that thimerosal alone does not activate IP_3R. Concentrations of thimerosal ($\leqslant 10$ μM) that cause substantial sensitization of IP_3R1 and IP_3R2 do not affect the Ca^{2+} content of the stores in the absence of IP_3 (Table 1). These results suggest

Table 3 Effects of thimerosal on binding of heparin and IP_3 dimer to the NT from IP_3R1

Equilibrium-competition binding experiments using [^{3}H]IP_3 (0.25 nM) and NT1 show the effects of thimerosal (100 μM, 10 min) on the K_d (mean), pK_d (mean $\pm$ S.E.M.) and Hill coefficient (h, mean $\pm$ S.E.M.) for IP_3 dimer and heparin. $\Delta pK_d = pK_d^{thimerosal} - pK_d^{control}$. Results are from $\geqslant$four independent experiments.

	pK_d (K_d) h		
	Control	Thimerosal	ΔpK_d
IP_3 dimer	9.81 $\pm$ 0.07 (0.15 nM) 1.2 $\pm$ 0.1	9.75 $\pm$ 0.14 (0.18 nM) 1.7 $\pm$ 0.4	$-$ 0.06 $\pm$ 0.19
Heparin	7.06 $\pm$ 0.09 (87 ng/ml) 0.82 $\pm$ 0.17	7.17 $\pm$ 0.03 (68 ng/ml) 0.73 $\pm$ 0.09	0.11 $\pm$ 0.09

that thimerosal might selectively stabilize an agonist-bound active conformation of IP_3R1.

Cysteine residues within both the SD and IBC are required for thimerosal to stimulate IP_3 binding

Previous work demonstrated that thimerosal stimulates [^{3}H]IP_3 binding to NT1, but not to the IBC [29]. Results shown in Figure 4 confirm that conclusion. We have shown that $NT1^{CL}$ is structurally and functionally indistinguishable from native NT1 [6]. The lack of effect of thimerosal on [^{3}H]IP_3 binding to $NT1^{CL}$ (Figure 4A) confirms that cysteine residues mediate its effects. We had anticipated, in keeping with earlier evidence [29], that cysteine residues within the SD were likely to mediate the effects of thimerosal. However, thimerosal had no effect on [^{3}H]IP_3 binding to NT lacking cysteine in either the SD ($NT1^{CL-SD}$) or the IBC ($NT1^{CL-IBC}$) (Figures 4B and 4C). These results demonstrate that stimulation of IP_3 binding by thimerosal requires cysteine residues within both the SD and IBC.

Residues within the NT are required for thimerosal to potentiate IP_3-evoked Ca^{2+} release

It would be instructive to examine the functional effects of thimerosal on full-length IP_3R1 in which cysteine residues within the NT are replaced by alanine and so verify whether the NT mediates the effects of thimerosal on IP_3-evoked Ca^{2+} release. We have demonstrated that IP_3R1 with a cysteine-less NT is functional, but only in transiently transfected DT40-KO cells [6], in which it is impracticable to complete the concentration–effect relationships needed to define the effects of thimerosal. We have not yet succeeded in establishing stable DT40 cell lines expressing IP_3R1 with a cysteine-less NT. We therefore adopted another approach and used a stable DT40 cell line expressing a chimaeric IP_3R1 in which the native SD is replaced by the equivalent region (the A domain) from a RyR (RyR1A-IP_3R1) [6] (Figure 5A, and Supplementary Table S1).

The A domain of RyR, which is structurally similar to the SD of IP_3R [6,48–50] (Supplementary Figure S1C and S1D), can functionally replace the SD of IP_3R1 to allow both IP_3-evoked Ca^{2+} release from a chimaeric IP_3R and appropriate regulation of IP_3 binding to a chimaeric NT [6]. All effective concentrations of thimerosal (1 μM–1 mM) inhibited [^{3}H]IP_3 binding to the chimaeric NT (RyR2A-IBC) (Figures 5A and 5B), although the effect appeared biphasic. Thimerosal (10 μM, 2 min)

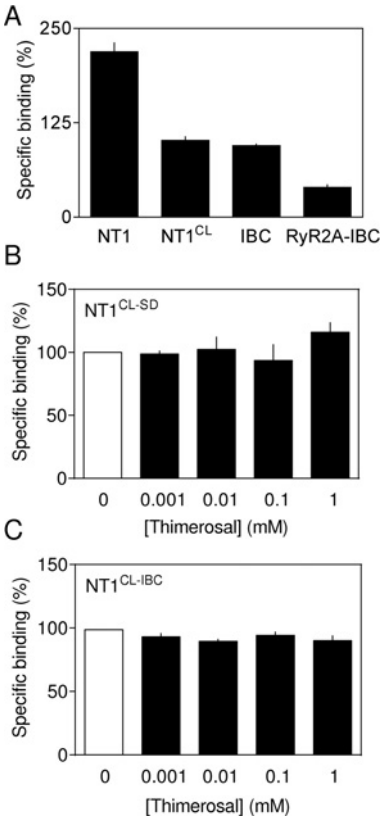

Figure 4 Stimulation of IP_3 binding by thimerosal requires cysteine residues within the SD and IBC

(**A**) Effects of thimerosal (100 μM, 10 min) on specific binding of [^{3}H]IP_3 (0.5 nM) to each of the indicated proteins. Results are expressed as a percentage of the binding measured in the absence of thimerosal. (**B** and **C**) Concentration-dependent effects of thimerosal on specific [^{3}H]IP_3 binding to $NT1^{CL-SD}$ (**B**) and $NT1^{CL-IBC}$ (**C**). All results are means $\pm$ S.E.M. for four independent experiments.

also inhibited IP_3-evoked Ca^{2+} release from the chimaeric IP_3R (RyR1A-IP_3R1) (Figure 5C and Table 1). These results suggest that these cysteine residues present within the SD of IP_3R1, but absent from the A domain of RyR, are required for thimerosal to potentiate IP_3-evoked Ca^{2+} release.

Conclusions

Thimerosal potentiates IP_3-evoked Ca^{2+} release via IP_3R1 and IP_3R2, but not via IP_3R3 (Figure 1). The parallel behaviour of NTs from each of the three IP_3R subtypes (Figure 2), our demonstration that cysteine residues are required within both the IBC and SD for thimerosal to stimulate IP_3 binding (Figure 4) and evidence that thimerosal does not potentiate responses from a chimaeric IP_3R1 in which the SD is replaced by the equivalent domain of a RyR (Figure 5) provide persuasive evidence that cysteine residues within the SD and IBC mediate functional responses to thimerosal. Furthermore, thimerosal selectively stimulates agonist, but not antagonist, binding to NT1 (Figure 3), suggesting that its interactions with critical cysteine residues selectively stabilize an active conformation of the NT. Because IP_3 binding rearranges interactions between the SD and IBC [6], this conclusion aligns with a previous suggestion that thimerosal stabilizes an interaction between the IBC and SD of IP_3R1 [29].

We do not know which specific cysteine residues are modified by thimerosal. Despite its subtype-selective actions (Figures 1 and 2) and evidence that sensitization by thimerosal is mediated

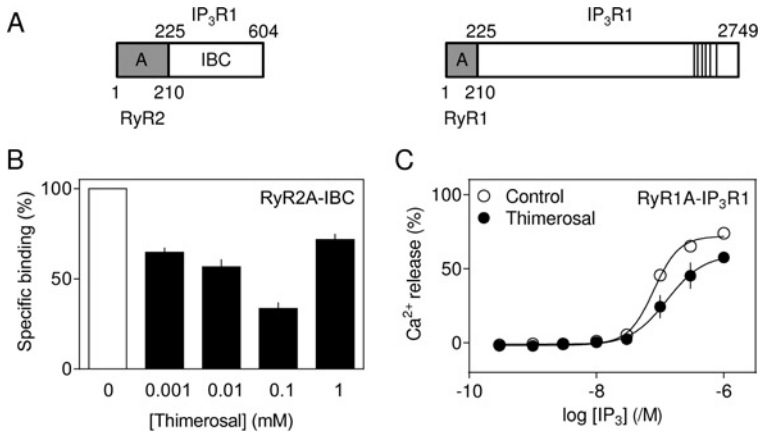

Figure 5 A chimaeric IP_3R1 is not stimulated by thimerosal

(**A**) The proteins used. (**B**) Concentration-dependent effects of thimerosal on specific [^{3}H]IP_3 (0.5 nM) binding to RyR2A-IBC. Results are expressed as percentages of the binding measured in the absence of thimerosal. (**C**) Concentration-dependent effects of IP_3 on Ca^{2+} release from DT40-RyR1A-IP_3R1 cells are shown for control cells and after treatment with thimerosal (10 μM, 2 min). Results in (**B** and **C**) are means $\pm$ S.E.M. from four independent experiments.

by cysteine residues within the NT, we have been unable to identify candidate cysteine residues from sequence data alone (see legend to Supplementary Figure S2 at http://www.biochemj.org/bj/451/bj4510177add.htm). Preliminary MALDI-TOF (matrix-assisted laser desorption ionization–time-of-flight) analyses were uninstructive, and it is impracticable to assay NT in which every pair of cysteine residues are mutated. It is perhaps surprising that cysteine residues in both the SD and IBC are required for thimerosal to sensitize IP_3R1. This requirement is unlikely to result from cross-linking of a pair of cysteine residues by thimerosal because available evidence suggests that thimerosal forms a mercuryethyl adduct with a single cysteine [24]. An alternative possibility is that thimerosal disrupts a disulfide bridge between cysteine residues in the SD and IBC that constrains IP_3R activation. This too seems unlikely. There is no evidence from the high-resolution structure of the NT for such a disulfide bridge [6]. Furthermore, IP_3R with cysteine-less NT are not constitutively active and respond normally to IP_3 [6]. We also used algorithms that predict the accessibility [51] and reactivity [52] of cysteine residues together with modelled structures of NT2–NT3 [53] to identify cysteine residues that might account for the differential sensitivities of IP_3R1–IP_3R3 to thimerosal. The results suggest that within the SD, there are two accessible cysteine residues (Cys^{206} and Cys^{214} in IP_3R1) and they are predicted to be equally accessible in all three subtypes, but the residue equivalent to Cys^{214} in IP_3R1 is less reactive in IP_3R3 (Supplementary Figure S2). Within the IBC, Cys^{556} is predicted to be accessible in IP_3R1 and IP_3R2, but it is buried in IP_3R3. Cys^{214} in the SD and Cys^{556} in the IBC of IP_3R1 therefore have the properties expected to explain the sensitization of IP_3R1 and IP_3R2, but not IP_3R3, by thimerosal. Further experimental work would be needed to assess this directly. We have provided the first systematic analysis of the effects of thiol reagents on each IP_3R subtype. We conclude that thimerosal sensitizes IP_3R1 and IP_3R2, but not IP_3R3, to IP_3. It does so by modifying cysteine residues within both the SD and IBC and thereby stabilizing an active conformation of the IP_3R.

AUTHOR CONTRIBUTION

Samir Khan completed most experimental analyses, with additional input from Ana Rossi. Andrew Riley and Barry Potter provided the IP_3 dimer. Colin Taylor designed the study, contributed to analysis of data and, with Ana Rossi, wrote the paper.

ACKNOWLEDGEMENTS

We thank Dr Saroj Velamakanni for assistance with some plasmids and Dr Taufiq Rahman for help with structural analysis.

FUNDING

This work was supported by grants from the Wellcome Trust [grant numbers 085295 (to C.W.T.) and 082837 (to B.V.L.P. and A.M.R.)] and Biotechnology and Biological Sciences Research Council (to C.W.T.). S.A.K. was funded by a Gates Nehru scholarship from the University of Cambridge. A.M.R. is a fellow at Queens' College, Cambridge.

REFERENCES

1 Taylor, C. W., Genazzani, A. A. and Morris, S. A. (1999) Expression of inositol trisphosphate receptors. Cell Calcium **26**, 237–251
2 Lanner, J. T., Georgiou, D. K., Joshi, A. D. and Hamilton, S. L. (2010) Ryanodine receptors: structure, expression, molecular details, and function in calcium release. Cold Spring Harbor Perspect. Biol. **2**, a003996
3 Xiao, B., Masumiya, H., Jiang, D., Wang, R., Yoshitatsu, S., Zhang, L., Murayama, T., Ogawa, Y., Lai, F. A., Wagenknecht, T. and Chen, S. R. W. (2002) Isoform dependent formation of heteromeric Ca^{2+} release channels (ryanodine receptors). J. Biol. Chem. **277**, 41778–41785
4 Bosanac, I., Alattia, J.-R., Mal, T. K., Chan, J., Talarico, S., Tong, F. K., Tong, K. I., Yoshikawa, F., Furuichi, T., Iwai, M. et al. (2002) Structure of the inositol 1,4,5-trisphosphate receptor binding core in complex with its ligand. Nature **420**, 696–700
5 Rossi, A. M., Riley, A. M., Tovey, S. C., Rahman, T., Dellis, O., Taylor, E. J. A., Veresov, V. G., Potter, B. V. L. and Taylor, C. W. (2009) Synthetic partial agonists reveal key steps in IP_3 receptor activation. Nat. Chem. Biol. **5**, 631–639
6 Seo, M.-D., Velamakanni, S., Ishiyama, N., Stathopulos, P. B., Rossi, A. M., Khan, S. A., Dale, P., Li, C., Ames, J. B., Ikura, M. and Taylor, C. W. (2012) Structural and functional conservation of key domains in $InsP_3$ and ryanodine receptors. Nature **483**, 108–112
7 Uchida, K., Miyauchi, H., Furuichi, T., Michikawa, T. and Mikoshiba, K. (2003) Critical regions for activation gating of the inositol 1,4,5-trisphosphate receptor. J. Biol. Chem. **278**, 16551–16560
8 Carney, J., Mason, S. A., Viero, C. and Williams, A. J. (2010) The ryanodine receptor pore: is there a consensus view? Curr. Top. Membr. **66**, 49–67
9 Foskett, J. K., White, C., Cheung, K. H. and Mak, D. O. (2007) Inositol trisphosphate receptor Ca^{2+} release channels. Physiol. Rev. **87**, 593–658
10 Laver, D. R. (2010) Regulation of RyR channel gating by Ca^{2+}, Mg^{2+} and ATP. Curr. Top. Membr. **66**, 69–89
11 Joseph, S. K. (2010) Role of thiols in the structure and function of inositol trisphosphate receptors. Curr. Top. Membr. **66**, 299–322

12 Meissner, G. (2010) Regulation of ryanodine receptor ion channels through posttranslational modifications. Curr. Top. Membr. **66**, 91–113
13 Hinman, A., Chuang, H. H., Bautista, D. M. and Julius, D. (2006) TRP channel activation by reversible covalent modification. Proc. Natl. Acad. Sci. U.S.A. **103**, 19564–19568
14 Scragg, J. L., Dallas, M. L., Wilkinson, J. A., Varadi, G. and Peers, C. (2008) Carbon monoxide inhibits L-type Ca^{2+} channels via redox modulation of key cysteine residues by mitochondrial reactive oxygen species. J. Biol. Chem. **283**, 24412–24419
15 Simon, F., Leiva-Salcedo, E., Armisen, R., Riveros, A., Cerda, O., Varela, D., Eguiguren, A. L., Olivero, P. and Stutzin, A. (2010) Hydrogen peroxide removes TRPM4 current desensitization conferring increased vulnerability to necrotic cell death. J. Biol. Chem. **285**, 37150–37158
16 Chuang, H. H. and Lin, S. (2009) Oxidative challenges sensitize the capsaicin receptor by covalent cysteine modification. Proc. Natl. Acad. Sci. U.S.A. **106**, 20097–20102
17 Bogeski, I., Kummerow, C., Al-Ansary, D., Schwarz, E. C., Koehler, R., Kozai, D., Takahashi, N., Peinelt, C., Griesemer, D., Bozem, M. et al. (2010) Differential redox regulation of ORAI ion channels: a mechanism to tune cellular calcium signaling. Sci. Signaling **3**, ra24
18 Madesh, M., Hawkins, B. J., Milovanova, T., Bhanumathy, C. D., Joseph, S. K., Ramachandrarao, S. P., Sharma, K., Kurosaki, T. and Fisher, A. B. (2005) Selective role for superoxide in $InsP_3$ receptor-mediated mitochondrial dysfunction and endothelial apoptosis. J. Cell Biol. **170**, 1079–1090
19 Campbell, D. L., Stamler, J. S. and Strauss, H. C. (1996) Redox modulation of L-type calcium channels in ferret ventricular myocytes. Dual mechanism regulation by nitric oxide and S-nitrosothiols. J. Gen. Physiol. **108**, 277–293
20 Viola, H. M., Arthur, P. G. and Hool, L. C. (2007) Transient exposure to hydrogen peroxide causes an increase in mitochondria-derived superoxide as a result of sustained alteration in L-type Ca^{2+} channel function in the absence of apoptosis in ventricular myocytes. Circ. Res. **100**, 1036–1044
21 Sun, Q. A., Hess, D. T., Nogueira, L., Yong, S., Bowles, D. E., Eu, J., Laurita, K. R., Meissner, G. and Stamler, J. S. (2011) Oxygen-coupled redox regulation of the skeletal muscle ryanodine receptor-Ca^{2+} release channel by NADPH oxidase 4. Proc. Natl. Acad. Sci. U.S.A. **108**, 16098–16103
22 Eu, J. P., Sun, J., Xu, L., Stamler, J. S. and Meissner, G. (2000) The skeletal muscle calcium release channel: coupled O_2 sensor and NO signaling functions. Cell **102**, 499–509
23 Baker, J. P. (2008) Mercury, vaccines, and autism: one controversy, three histories. Am. J. Public Health **98**, 244–253
24 Elferink, J. G. (1999) Thimerosal: a versatile sulfhydryl reagent, calcium mobilizer, and cell function-modulating agent. Gen. Pharmacol. **33**, 1–6
25 Tanaka, Y. and Tashjian, Jr, A. H. (1994) Thimerosal potentiates Ca^{2+} release mediated by both the inositol 1,4,5-trisphosphate and the ryanodine receptors in sea urchin eggs. Implications for mechanistic studies on Ca^{2+} signaling. J. Biol. Chem. **269**, 11247–11253
26 Aracena-Parks, P., Goonasekera, S. A., Gilman, C. P., Dirksen, R. T., Hidalgo, C. and Hamilton, S. L. (2006) Identification of cysteines involved in S-nitrosylation, S-glutathionylation, and oxidation to disulfides in ryanodine receptor type 1. J. Biol. Chem. **281**, 40354–40368
27 Lock, J. T., Sinkins, W. G. and Schilling, W. P. (2012) Protein S-glutathionylation enhances Ca^{2+}-induced Ca^{2+} release via the IP_3 receptor in cultured aortic endothelial cells. J. Physiol. **590**, 3431–3447
28 Lock, J. T., Sinkins, W. G. and Schilling, W. P. (2011) Effect of protein S-glutathionylation on Ca^{2+} homeostasis in cultured aortic endothelial cells. Am. J. Physiol. **300**, H493–H506
29 Bultynck, G., Szlufcik, K., Kasri, N. N., Assefa, Z., Callewaert, G., Missiaen, L., Parys, J. B. and De Smedt, H. (2004) Thimerosal stimulates Ca^{2+} flux through inositol 1,4,5-trisphosphate receptor type 1, but not type 3, via modulation of an isoform-specific Ca^{2+}-dependent intramolecular interaction. Biochem. J. **381**, 87–96
30 Higo, T., Hattori, M., Nakamura, T., Natsume, T., Michikawa, T. and Mikoshiba, K. (2005) Subtype-specific and ER lumenal environment-dependent regulation of inositol 1,4,5-trisphosphate receptor type 1 by ERp44. Cell **120**, 85–98
31 Tovey, S. C., Sun, Y. and Taylor, C. W. (2006) Rapid functional assays of intracellular Ca^{2+} channels. Nat. Protoc. **1**, 259–263
32 Rossi, A. M. and Taylor, C. W. (2011) Analysis of protein-ligand interactions by fluorescence polarization. Nat. Protoc. **6**, 365–387
33 Otsu, K., Willard, H. F., Khanna, V. K., Zorzato, F., Green, N. M. and MacLennan, D. H. (1990) Molecular cloning of cDNA encoding the Ca^{2+} release channel (ryanodine receptor) of rabbit cardiac muscle sarcoplasmic reticulum. J. Biol. Chem. **265**, 13472–13483
34 Tovey, S., Dedos, S. G., Taylor, E. J. A., Church, J. E. and Taylor, C. W. (2008) Selective coupling of type 6 adenylyl cyclase with type 2 IP_3 receptors mediates a direct sensitization of IP_3 receptors by cAMP. J. Cell Biol. **183**, 297–311
35 Iwai, M., Michikawa, T., Bosanac, I., Ikura, M. and Mikoshiba, K. (2007) Molecular basis of the isoform-specific ligand-binding affinity of inositol 1,4,5-trisphosphate receptors. J. Biol. Chem. **282**, 12755–12764
36 Bootman, M. D., Taylor, C. W. and Berridge, M. J. (1992) The thiol reagent, thimerosal, evokes Ca^{2+} spikes in HeLa cells by sensitizing the inositol 1,4,5-trisphosphate receptor. J. Biol. Chem. **267**, 25113–25119
37 Kaplin, A. I., Ferris, C. D., Voglmaier, S. M. and Snyder, S. H. (1994) Purified reconstituted inositol 1,4,5-trisphosphate receptors: thiol reagents act directly on receptor protein. J. Biol. Chem. **269**, 28972–28978
38 Thorn, P., Brady, P., Llopis, J., Gallacher, D. V. and Petersen, O. H. (1992) Cytosolic Ca^{2+} spikes evoked by the thiol reagent thimerosal in both intact and internally perfused single pancreatic acinar cells. Pflügers Arch. **422**, 173–178
39 Islam, M. S., Rorsman, P. and Berggren, P. O. (1992) Ca^{2+}-induced Ca^{2+} release in insulin-secreting cells. FEBS J. **296**, 287–291
40 Missiaen, L., Taylor, C. W. and Berridge, M. J. (1992) Luminal Ca^{2+} promoting spontaneous Ca^{2+} release from inositol trisphosphate-sensitive stores of rat hepatocytes. J. Physiol. **455**, 623–640
41 Missiaen, L., Parys, J. B., Sienaert, I., Maes, K., Kunzelmann, K., Takahashi, M., Tanzawa, K. and De Smedt, H. (1998) Functional properties of the type-3 $InsP_3$ receptor in 16HBE14o- bronchial mucosal cells. J. Biol. Chem. **273**, 8983–8986
42 Mezna, M. and Michelangeli, F. (1997) Effects of thimerosal on the transient kinetics of inositol 1,4,5-trisphosphate-induced Ca^{2+} release from cerebellar microsomes. Biochem. J. **325**, 177–182
43 Renard, D. C., Seitz, M. B. and Thomas, A. P. (1992) Oxidized glutathione causes sensitization of calcium release to inositol 1,4,5-trisphosphate in permeabilized hepatocytes. Biochem. J. **284**, 507–512
44 Bird, G. S. J., Burgess, G. M. and Putney, Jr, J. W. (1993) Sulfhydryl reagents and cAMP-dependent protein kinase increase the sensitivity of the inositol 1,4,5-trisphosphate receptor in hepatocytes. J. Biol. Chem. **268**, 17917–17923
45 Vanlingen, S., Sipma, H., Missiaen, L., De Smedt, H., De Smet, P., Casteels, R. and Parys, J. B. (1999) Modulation of type 1, 2 and 3 inositol 1,4,5,-trisphosphate receptors by cyclic ADP-ribose and thimerosal. Cell Calcium **25**, 107–114
46 Vanlingen, S., Sipma, H., De Smet, P., Callewaert, G., Missiaen, L., De Smedt, H. and Parys, J. B. (2001) Modulation of inositol 1,4,5-trisphosphate binding to the various inositol 1,4,5-trisphosphate receptor isoforms by thimerosal and cyclic ADP-ribose. Biochem. Pharmacol. **61**, 803–809
47 Ghosh, T. K., Eis, P. S., Mullaney, J. M., Ebert, C. L. and Gill, D. L. (1988) Competitive, reversible, and potent antagonism of inositol 1,4,5-trisphosphate-activated calcium release by heparin. J. Biol. Chem. **263**, 11075–11079
48 Amador, F. J., Liu, S., Ishiyama, N., Plevin, M. J., Wilson, A., Maclennan, D. H. and Ikura, M. (2009) Crystal structure of type I ryanodine receptor amino-terminal β-trefoil domain reveals a disease-associated mutation 'hot spot' loop. Proc. Natl. Acad. Sci. U.S.A. **106**, 11040–11044
49 Lobo, P. A. and Van Petegem, F. (2009) Crystal structures of the N-terminal domains of cardiac and skeletal muscle ryanodine receptors: insights into disease mutations. Structure **17**, 1505–1514
50 Tung, C. C., Lobo, P. A., Kimlicka, L. and Van Petegem, F. (2010) The amino-terminal disease hotspot of ryanodine receptors forms a cytoplasmic vestibule. Nature **585**, 585–588
51 Li, H., Robertson, A. D. and Jensen, J. H. (2005) Very fast empirical prediction and rationalization of protein pKa values. Proteins **61**, 704–721
52 Jacob, M. H., Amir, D., Ratner, V., Gussakowsky, E. and Haas, E. (2005) Predicting reactivities of protein surface cysteines as part of a strategy for selective multiple labeling. Biochemistry **44**, 13664–13672
53 Saleem, H., Tovey, S. C., Rahman, T., Riley, A. M., Potter, B. V. L. and Taylor, C. W. (2012) Stimulation of inositol 1,4,5-trisphosphate (IP_3) receptor subtypes by analogues of IP_3. PLoS ONE **8**, e54877

Received 18 October 2012/3 December 2012; accepted 2 January 2012
Published as BJ Immediate Publication 2 January 2013, doi:10.1042/BJ20121600

Biochem. J. (2013) **451**, 177–184 (Printed in Great Britain) doi:10.1042/BJ20121600

online data

SUPPLEMENTARY ONLINE DATA

Subtype-selective regulation of IP_3 receptors by thimerosal via cysteine residues within the IP_3-binding core and suppressor domain

Samir A. KHAN*[1], Ana M. ROSSI*[1], Andrew M. RILEY†, Barry V. L. POTTER† and Colin W. TAYLOR*[2]

*Department of Pharmacology, Tennis Court Road, Cambridge CB2 1PD, U.K., and †Wolfson Laboratory of Medicinal Chemistry, Department of Pharmacy and Pharmacology, University of Bath, Claverton Down, Bath BA2 7AY, U.K.

Table S1 Proteins used and their abbreviations

Abbreviations	Protein
IP_3R1	Full-length rat IP_3R1 lacking S1 splice region (GenBank: GQ233032.1)
IP_3R2	Full-length mouse IP_3R2 (GenBank: GU980658.1)
IP_3R3	Full-length rat IP_3R3 (GenBank: GQ233031.1)
RyR1A-IP_3R1	Full-length rat IP_3R1 (GenBank: GQ233032.1) with residues 1–224 replaced by residues 1–210 from rabbit RyR1 (GenBank: X15209)
NT1	Residues 1–604 from rat IP_3R1
NT2	Residues 1–604 from mouse IP_3R2
NT3	Residues 1–604 from rat IP_3R3
IBC	Residues 224–604 from rat IP_3R1
$NT1^{CL}$	Residues 1–604 from rat IP_3R1 with all cysteine residues replaced by alanine
$NT1^{CL-SD}$	Residues 1–604 from rat IP_3R1 with all cysteine residues within the SD (residues 1–223) replaced by alanine
$NT1^{CL-IBC}$	Residues 1–604 from rat IP_3R1 with all cysteine residues within the IBC (residues 224–604) replaced by alanine
RyR2A-IBC	Residues 1–604 from rat IP_3R1 with residues 1-224 replaced by residues 1–210 from rabbit RyR2 (GenBank: GI164831)

Table S2 Primers used

Sequences of the forward (F) and reverse (R) primers used to amplify by PCR the sequences encoding the constructs used. Other primers have been specified in earlier publications [1,2].

Construct	Direction	Sequence (5′–3′)
NT2	F	GGCCCCCGGGATGTCTGACAAAATGTCCAGCTTCCTCTACATTGGG
	R	GGCCCTCGAGTTATTTGCGGTTGTTGTGTAACAAGGCTGTAATCGT
NT3	F	GGCCCCCGGGATGAATGAAATGTCCAGCTTTCTTCACATCGGGGAC
	R	GGCCCTCGAGTTACTTCCGGTTGTTGTGCAGCAGGGC CGTGATGGT
$NT1^{CL-SD}$	F	ACTAGTATGTCTGACAAAATGTCTAGTTTCCT
	R	GATATCGAAAAGCACTATTTTCCAGCTTG

[1] These authors contributed equally to this work.
[2] To whom correspondence should be addressed (email cwt1000@cam.ac.uk).

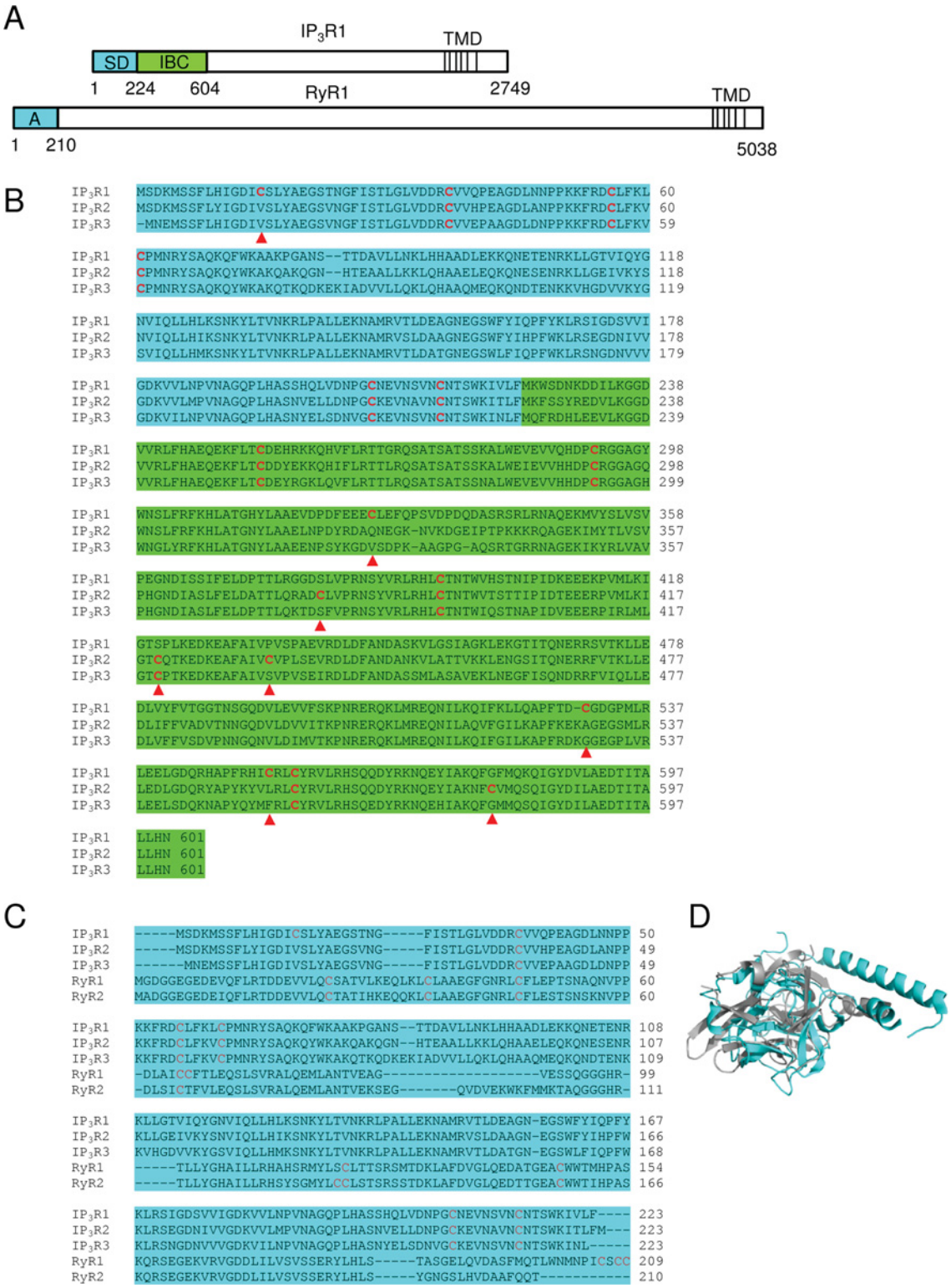

Figure S1 Comparison of key sequences between IP_3R subtypes and RyR

(**A**) Key domains of a single subunit of rat IP_3R1 and rabbit RyR1 shown to highlight locations of the SD and A domain. (**B**) Sequence alignment (Clustal) of the three IP_3R subtypes. Cyan shows the SD and green shows the IBC. Red arrowheads highlight cysteine residues that differ between IP_3R subtypes. (**C**) Sequence alignment (Clustal) of the SD of the three IP_3R subtypes and A domains of RyR1 and RyR2. (**D**) Structural alignments (Pymol) of the SD of IP_3R1 (cyan; PDB 1XZZ) and A domain of RyR2 (grey; PDB 3IM5).

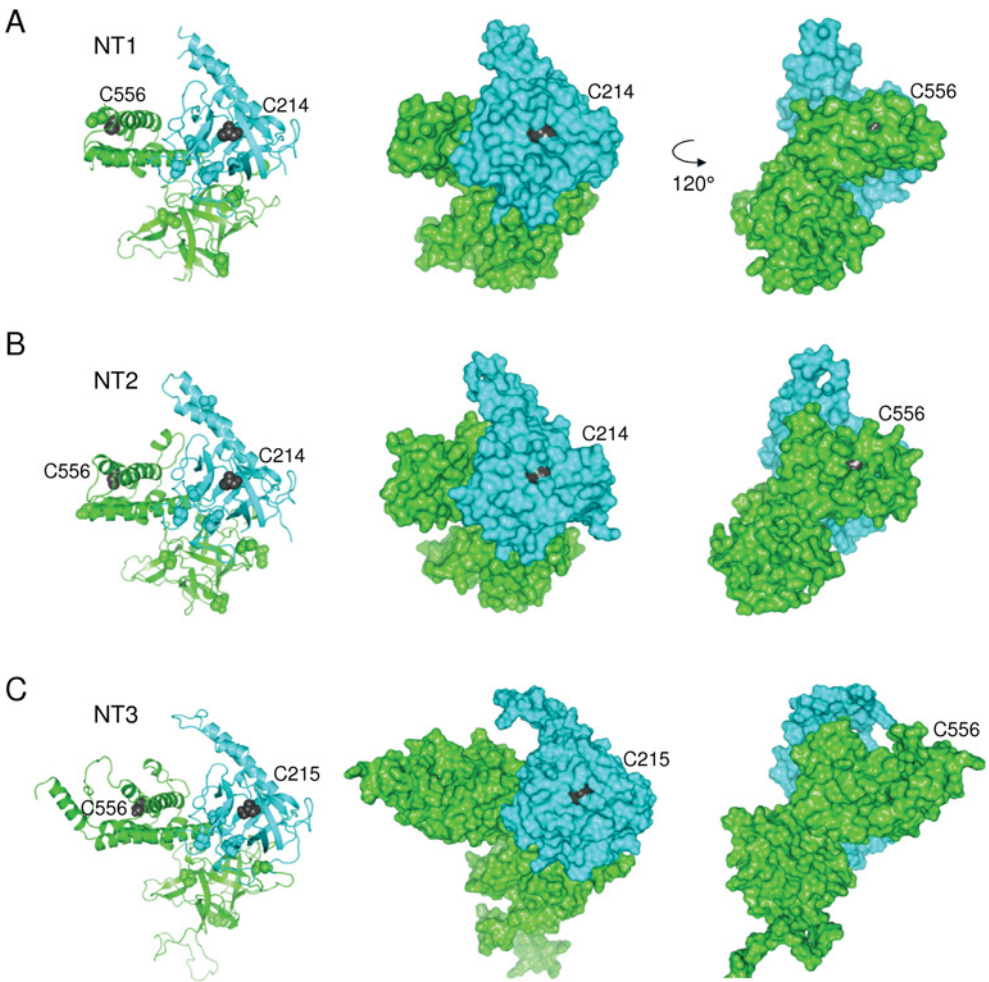

Figure S2 Differences in the accessibility and reactivity of cysteine residues within the NT of IP_3R subtypes may account for their differential regulation by thimerosal

(**A**–**C**) Structural homology models [3] of NT2 and NT3 on the basis of the known structure of $NT1^{CL}$ (PDB 3UJ4) [2] with the native cysteine restored (using Pymol). The structures show the SD (cyan) and IBC (green) and the positions of all cysteine residues. Thimerosal increases the sensitivity to IP_3 of IP_3R1 and IP_3R2, but not of IP_3R3 (Figure 1 of the main text), and its actions require cysteine residues within the NT (Figures 4 and 5 of the main text). We therefore considered whether residues conserved within the SD and IBC of IP_3R1 and IP_3R2, but absent from IP_3R3, might be responsible. There are six cysteine residues within the SD of IP_3R1, two of these (Cys^{56} and Cys^{61}) are not required for thimerosal to stimulate IP_3 binding [4], and five of the residues are conserved in all three IP_3R subtypes. The remaining cysteine residue (Cys^{15}) is unique to IP_3R1. The IBC of the IP_3R1 used in the present study (where the S1 splice site, which includes Cys^{326}, is removed) has six cysteine residues, four of which are conserved, but the remaining two (Cys^{530} and Cys^{553}) are unique to IP_3R1. There are therefore no cysteine residues in the NT that are uniquely conserved in IP_3R1 and IP_3R2. Replacing the SD of IP_3R1 with the A domain of RyR1 caused thimerosal to become inhibitory, suggesting that cysteine residues present in the SD, but absent from the A domain, might contribute to the stimulatory effect of thimerosal. Two of the six cysteine residues within the SD (Cys^{36} and Cys^{56}) are conserved in all three IP_3R subtypes, RyR1 and RyR2, and are therefore unlikely to mediate stimulation of IP_3R1 by thimerosal. None of the remaining four cysteine residues in the SD are present in the A domain, but neither are they uniquely shared with IP_3R2. We were therefore unable to identify from these sequence comparisons alone the cysteine residues within the NT that are likely to mediate the stimulatory effect of thimerosal. The reactivity of a cysteine residue depends on its accessibility and whether it is deprotonated [5,6]. Using the NT1–NT3 structures, two cysteine residues were identified that would be expected to be reactive in NT1 and NT2, but non-reactive in NT3. These residues are highlighted (grey) in the structures and their surface accessibility is shown in the right-hand panels.

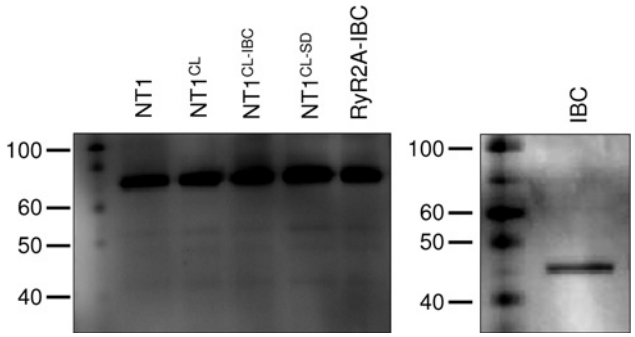

Figure S3 Expression of NT fragments of IP_3R

Immunoblots of the indicated purified fragments (3 μg/lane), using AbC, which recognizes a sequence conserved in all IP_3R subtypes (residues 240–253 of rat IP_3R1). Molecular mass markers are shown on the left in kDa.

REFERENCES

1 Rossi, A. M., Riley, A. M., Tovey, S. C., Rahman, T., Dellis, O., Taylor, E. J. A., Veresov, V. G., Potter, B. V. L. and Taylor, C. W. (2009) Synthetic partial agonists reveal key steps in IP_3 receptor activation. Nat. Chem. Biol. **5**, 631–639

2 Seo, M.-D., Velamakanni, S., Ishiyama, N., Stathopulos, P. B., Rossi, A. M., Khan, S. A., Dale, P., Li, C., Ames, J. B., Ikura, M. and Taylor, C. W. (2012) Structural and functional conservation of key domains in $InsP_3$ and ryanodine receptors. Nature **483**, 108–112

3 Saleem, H., Tovey, S. C., Rahman, T., Riley, A. M., Potter, B. V. L. and Taylor, C. W. (2012) Stimulation of inositol 1,4,5-trisphosphate (IP_3) receptor subtypes by analogues of IP_3. PLoS ONE **8**, e54877

4 Bultynck, G., Szlufcik, K., Kasri, N. N., Assefa, Z., Callewaert, G., Missiaen, L., Parys, J. B. and De Smedt, H. (2004) Thimerosal stimulates Ca^{2+} flux through inositol 1,4,5-trisphosphate receptor type 1, but not type 3, via modulation of an isoform-specific Ca^{2+}-dependent intramolecular interaction. Biochem. J. **381**, 87–96

5 Li, H., Robertson, A. D. and Jensen, J. H. (2005) Very fast empirical prediction and rationalization of protein pKa values. Proteins **61**, 704–721

6 Jacob, M. H., Amir, D., Ratner, V., Gussakowsky, E. and Haas, E. (2005) Predicting reactivities of protein surface cysteines as part of a strategy for selective multiple labeling. Biochemistry **44**, 13664–13672

Received 18 October 2012/3 December 2012; accepted 2 January 2012
Published as BJ Immediate Publication 2 January 2013, doi:10.1042/BJ20121600